


RESEARCH

Open Access



# Serum- and xeno-free culture of human umbilical cord perivascular cells for pediatric heart valve tissue engineering

Shouka Parvin Nejad<sup>1,2\*</sup>, Monica Lecce<sup>1,2</sup>, Bahram Mirani<sup>1,2,3</sup>, Nataly Machado Siqueira<sup>1,2</sup>, Zahra Mirzaei<sup>1,3</sup>, J. Paul Santerre<sup>1,2,4</sup>, John E. Davies<sup>2,4,5</sup> and Craig A. Simmons<sup>1,2,3\*</sup> 

## Abstract

**Background** Constructs currently used to repair or replace congenitally diseased pediatric heart valves lack a viable cell population capable of functional adaptation in situ, necessitating repeated surgical intervention. Heart valve tissue engineering (HVTE) can address these limitations by producing functional living tissue in vitro that holds the potential for somatic growth and remodelling upon implantation. However, clinical translation of HVTE strategies requires an appropriate source of autologous cells that can be non-invasively harvested from mesenchymal stem cell (MSC)-rich tissues and cultured under serum- and xeno-free conditions. To this end, we evaluated human umbilical cord perivascular cells (hUCPVCs) as a promising cell source for in vitro production of engineered heart valve tissue.

**Methods** The proliferative, clonogenic, multilineage differentiation, and extracellular matrix (ECM) synthesis capacities of hUCPVCs were evaluated in a commercial serum- and xeno-free culture medium (StemMACS™) on tissue culture polystyrene and benchmarked to adult bone marrow-derived MSCs (BMMSCs). Additionally, the ECM synthesis potential of hUCPVCs was evaluated when cultured on polycarbonate polyurethane anisotropic electrospun scaffolds, a representative biomaterial for in vitro HVTE.

**Results** hUCPVCs had greater proliferative and clonogenic potential than BMMSCs in StemMACS™ ( $p < 0.05$ ), without differentiation to osteogenic and adipogenic phenotypes associated with valve pathology. Furthermore, hUCPVCs cultured with StemMACS™ on tissue culture plastic for 14 days synthesized significantly more total collagen, elastin, and sulphated glycosaminoglycans ( $p < 0.05$ ), the ECM constituents of the native valve, than BMMSCs. Finally, hUCPVCs retained their ECM synthesizing capacity after 14 and 21 days in culture on anisotropic electrospun scaffolds.

**Conclusion** Overall, our findings establish an in vitro culture platform that uses hUCPVCs as a readily-available and non-invasively sourced autologous cell population and a commercial serum- and xeno-free culture medium to increase the translational potential of future pediatric HVTE strategies.

**Keywords** Mesenchymal stromal cells, Human umbilical cord perivascular cells, Serum- and xeno-free culture, Extracellular matrix, Heart valve tissue engineering

\*Correspondence:

Shouka Parvin Nejad  
shouka.parvinnejad@mail.utoronto.ca

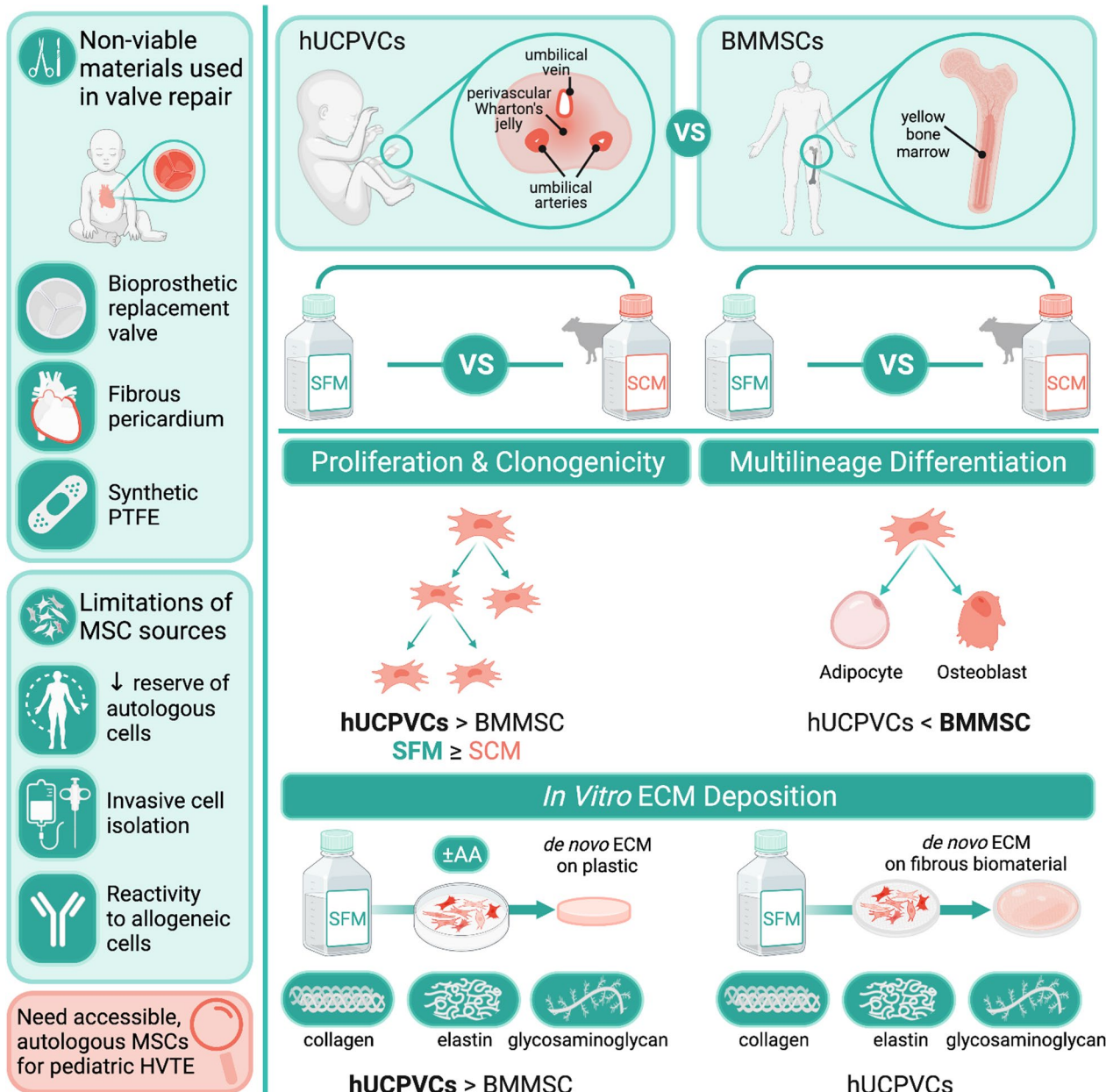
Craig A. Simmons  
c.simmons@utoronto.ca

Full list of author information is available at the end of the article



© The Author(s) 2023. **Open Access** This article is licensed under a Creative Commons Attribution 4.0 International License, which permits use, sharing, adaptation, distribution and reproduction in any medium or format, as long as you give appropriate credit to the original author(s) and the source, provide a link to the Creative Commons licence, and indicate if changes were made. The images or other third party material in this article are included in the article's Creative Commons licence, unless indicated otherwise in a credit line to the material. If material is not included in the article's Creative Commons licence and your intended use is not permitted by statutory regulation or exceeds the permitted use, you will need to obtain permission directly from the copyright holder. To view a copy of this licence, visit <http://creativecommons.org/licenses/by/4.0/>. The Creative Commons Public Domain Dedication waiver (<http://creativecommons.org/publicdomain/zero/1.0/>) applies to the data made available in this article, unless otherwise stated in a credit line to the data.

Graphical Abstract



This study evaluated the proliferative, differentiation and extracellular matrix (ECM) synthesis capacities of human umbilical cord perivascular cells (hUCPVCs) when cultured in serum- and xeno-free media (SFM) against conventionally used bone marrow-derived MSCs (BMMSCs) and serum-containing media (SCM). Our findings support the use of hUCPVCs and SFM for in vitro heart valve tissue engineering (HVTE) of autologous pediatric valve tissue. Figure created with BioRender.com.

Introduction

Despite significant advances in interventional cardiology and cardiac surgery [1, 2], valvular repair and

replacement procedures still cannot ensure long-term functionality and freedom from reoperation for pediatric patients with congenital heart defects (CHDs), largely

because of deficits inherent to valve repair materials and prosthetic replacement valves themselves. In particular, the lack of a viable cell population associated with these interventions renders them incapable of somatic growth, repair, and functional adaptation in response to changing biochemical and biomechanical cues.

Heart valve tissue engineering (HVTE) holds the potential to resolve the currently unmet need for valvular repair and replacement tissue that can grow, self-repair, and remodel to support life-long performance. HVTE strategies can be broadly stratified into *in vitro*, *in situ*, and *in vivo* HVTE, with the former two being the most prevalent approaches [3, 4]. *In vitro* HVTE strategies couple resorbable biomaterials and stromal cells with the aim of producing cellularised living replacement neo-tissue with the compositional, architectural and mechanical properties to function *in vivo*. While the biomaterial provides a structurally and mechanically robust scaffolding on which extracellular matrix (ECM) is deposited, the presence of a viable cell population in tissue engineered heart valves (TEHVs) ensures functional adaptation and remodelling of the ECM, analogous to the valvular interstitial cell population resident within the native valve [5]. *In situ* TEHVs encompass bioengineered valve replacements that are decellularized prior to implantation and rely on infiltration of endogenous host cells to populate the construct *in vivo*. *In situ* strategies most often use decellularized *in vitro* TEHVs, and less frequently, acellular bioresorbable scaffolds or decellularized allogeneic or xenogeneic valves. Thus, all *in vitro* and a majority of *in situ* HVTE strategies are entirely contingent on the stromal cell source to synthesize structural ECM proteins and assemble tissue *in vitro*.

HVTE strategies have historically used mesenchymal stromal cells (MSCs) sourced from vascular, dermal, adipose and bone marrow tissues, as they resemble the fibroblast subpopulation of the native valve and can undergo myofibrogenesis to synthesize the three main constituent ECM proteins of the valve leaflet: collagen, elastin, and glycosaminoglycans [6–9]. In the context of pediatric HVTE, MSCs derived from conventional tissue sources are constrained by at least one of three limitations: (i) the invasive nature of cell isolation; (ii) a limited reserve of autologous MSCs; and (iii) immunogenicity associated with allogeneic major histocompatibility complex I-mismatched MSCs [10, 11]. Thus, fetal MSCs derived from prenatal (amniotic fluid, amniotic membrane) and early postnatal (placenta, umbilical cord blood, umbilical cord matrix) tissues have been studied for their utility to pediatric HVTE [12–14].

Among fetal sources of MSCs, the umbilical cord is a promising candidate, as a rich source of autologous progenitor cells that can be harvested non-invasively

from tissue that is typically discarded. Human umbilical cord perivascular cells (hUCPVCs) harvested from the perivascular region of the Wharton's jelly (WJ) possess characteristic properties of MSCs [15–17] in accordance with the minimal criteria set by the International Society for Cell and Gene Therapy (ISCT) MSC committee [18] - hUCPVCs are plastic adherent, differentiate to osteogenic, adipogenic and chondrogenic lineages, and present appropriate cell surface markers (CD105+, CD73+, CD90+, CD45–, CD34–, CD14–, HLA-DR–) [16, 19–21]. Additionally, hUCPVCs contain a high frequency of colony forming unit-fibroblasts (CFU-F) that maintain proliferative and multilineage differentiation potential [22]. Their proven regenerative capacity in dermal wound healing [23], musculoskeletal repair [22], and acute myocardial infarction [16] make a compelling case for their use as autologous progenitor cells for pediatric HVTE. While *in vitro* cardiovascular tissue engineering strategies have taken advantage of umbilical cord-derived MSCs to synthesize neo-tissue [24–30], these findings cannot be projected to hUCPVCs due to a lacking consensus in the literature with respect to both the anatomical descriptors of the specific regions from which umbilical cord MSCs were harvested and the methodological techniques used to harvest these cells. Furthermore, previous studies of umbilical cord-derived MSCs for *in vitro* cardiovascular tissue engineering have been conducted in xenogenic serum-supplemented culture conditions, complicating their translational potential.

Clinical translation of TEHVs produced from the combination of biomaterial scaffolds and hUCPVCs ultimately necessitates reproducible *in vitro* culture conditions. However, supplementation of cell culture medium with undefined xenogenic serum poses a challenge to good manufacturing practices (GMP) as (i) xenogenic serum-containing media (SCM) carries an inherent risk of viral, bacterial, or prion disease transmission from the donor to culture adapted human MSCs [31, 32]; (ii) the presence of xenogenic proteins in engineered constructs cultured with serum can provoke an immune response in a human recipient, undermining the use of autologous cells [33]; and (iii) the undefined composition of serum and lot-to-lot variability resulting from differences in animal husbandry can induce variable responses in culture adapted cells [34, 35].

Here we report serum- and xeno-free culture of hUCPVCs for *in vitro* HVTE applications and benchmark them against human bone marrow-derived MSCs (BMMSCs), the most pervasively used MSCs in regenerative applications. We show that a commercially available serum- and xeno-free culture medium supports the proliferative capacity of hUCPVCs and BMMSCs and establish serum- and xeno-free *in vitro* culture conditions to

promote deposition of the ECM proteins critical to the structure and function of valve tissue (collagen, elastin, and glycosaminoglycans). Finally, we confirm ECM synthesis by hUCPVCs on electrospun scaffold sheets in a preliminary study of engineered PV repair constructs. This study establishes hUCPVCs as a suitable cell source for HVTE, supported by their accessibility, rapid proliferation, and capacity to generate neo-tissue under serum- and xeno-free culture conditions.

## Materials and Methods

### Cell sources and expansion

Adult human BMMSCs from three male donors were used in this study. BMMSCs from one donor were obtained at passage 1 from Texas A&M Health Science Centre College of Medicine Institute for Regenerative Medicine at Scott & White through a grant from ORIP of the NIH, grant #P40OD011050 (Donor #8013L). Cells were subsequently expanded to passage 5 in SCM consisting of *a*-MEM (Gibco™, cat #12483-020) supplemented with 2–4 mM L-glutamine (Sigma-Aldrich, cat #G7513), 16.7% fetal bovine serum (Gibco™, cat #12561-056), and 1% penicillin/streptomycin (Life Technologies, cat #15140122). BMMSCs from Donor #8013L were used at passage 5 for all experiments. BMMSCs from the remaining two donors were obtained at passage 1 from Lonza (cat #PT-2501, Donor #36461 and Donor #36550) and expanded to passage 3 using MSCGM™ Stem Cell Growth Media Bullekit (Lonza, cat #PT-3001) as per the vendor's recommendations. BMMSCs from Donor #36461 and Donor #36550 were used at passage 3 for all experiments. hUCPVCs from full-term umbilical cords of three male neonatal donors (Donor #0917003; Donor #0917004; and Donor #0317004) were isolated and expanded by Tissue Regeneration Therapeutics Inc. (Toronto, Ontario, Canada) using a proprietary protocol and provided in-kind at passage 1. hUCPVCs were expanded to passage 3 using StemMACS™ MSC Expansion Media Kit XF (henceforth referred to as StemMACS™) (Miltenyi Biotec, cat #130-104-182) supplemented with 5 mL of a concentrated antibiotic cocktail consisting of 0.6 mg amphotericin-B (Sigma cat #A9528), 200 mg penicillin (Bioshop Canada, cat #PEN333.25), 100 mg gentamicin sulfate (Sigma, cat #G1397) in 20 mL of phosphate buffered saline (PBS). hUCPVCs from all three donors were used at passage 3 for all experiments.

### Proliferation in StemMACS™

hUCPVCs and BMMSCs from each donor were seeded in 6-well tissue culture plates in triplicate at a density of 3000 cells/cm<sup>2</sup> and cultured in either StemMACS™ or SCM. Cell culture media was refreshed every three days. Cells were cultured to specific time-points (2, 4, 6, and 8 days in

culture) before dissociation by TrypLE (Gibco™, cat # 12604021) and 125 CDU/mL collagenase (Sigma, cat #C0130). Harvested cells were subsequently stained with trypan blue and viable cells were manually counted using a hemocytometer. Average population doubling time over 6 days (day 2–8) was calculated using the following equation: Doubling Time(hrs) =  $t * (\log(2)) / \log\left(\frac{N_t}{N_0}\right)$ , where  $N_0$  is the average number of live cells harvested from one well of a 6-well plate on day 2 and  $N_t$  is the number of live cells after 8 days of culture.

### CFU-F frequency in StemMACS™

hUCPVCs and BMMSCs from each donor were cultured in T25 culture flasks in either StemMACS™ or SCM. Once cells reached 75–80% confluence (assessed visually) they were detached from culture flasks by TrypLE, resuspended in either StemMACS™ or SCM, and subsequently plated at a density of 100 cells/well in 6-well tissue culture plates in triplicate. On day 7, samples were washed with PBS, stained with 2.5% crystal violet in 100% ethanol for 1 h at room temperature, and rinsed with distilled water. Stained colonies were first visually identified in the wells and counted as a colony upon confirmation of 8 or more cells within the cluster using brightfield microscopy.

### Osteogenic and adipogenic differentiation potential

Osteogenic and adipogenic differentiation potential were assessed in accordance with the ISCT minimal criteria for MSCs [18]. hUCPVCs and BMMSCs from each donor were seeded in 6-well tissue culture plates at a density of 3000 cells/cm<sup>2</sup> with SCM. At 75–80% confluence (assessed visually), cell culture media was replaced with either osteogenic induction media, adipogenic induction media, or control SCM. Each cell donor was cultured in triplicate under each media condition. Osteogenic differentiation medium consisted of SCM supplemented 10 nM dexamethasone (Sigma, cat #D2915), 20 μM β-glycerolphosphate (Sigma, cat #G9891), and 50 μM L-ascorbic acid 2-phosphate (Sigma, cat #A8960). Adipogenic differentiation medium consisted of SCM supplemented with 0.5 μM dexamethasone (Sigma, cat #D2915), 0.5 μM isobutylmethylxanthine (Sigma, cat #I5879), and 50 μM indomethacin (Sigma, cat #I7378). Cells were cultured for up to 20 days after induction, and media was refreshed every 4 days. Due to cell peeling and rolling, hUCPVCs from one biological donor (Donor #0917004) were fixed on day 15 of induction with differentiation medium. Cells were fixed with 10% neutral buffered formalin (NBF) (Sigma, cat #HT501128) and stored in PBS at 4 °C prior to staining. Osteogenic and adipogenic differentiation was assessed by staining



with 2% alizarin red solution (Electron Microscopy Sciences, cat #2620601) and 0.3% (w/v) oil red-O (Sigma, cat #00625) solution respectively, using a protocol provided by Texas A&M Health Science Centre College of Medicine Institute for Regenerative Medicine.

### ECM protein synthesis

hUCPVCs and BMMSCs from each donor were seeded in 12-well tissue culture plates with StemMACS™ cell culture media at a density of 3000 cells/cm<sup>2</sup>. Cell culture media was changed on day 1 and replaced with either StemMACS™ or 50 μM ascorbic acid (AA) (Sigma, cat #A4544) supplemented StemMACS™. Cell culture media was refreshed every 1–2 days. AA-supplemented culture media was prepared fresh at each media change. Cells were cultured for 14 days. Due to observations of cell peeling and rolling among the BMMSC donors, samples were harvested after 9 (Donor #36461 and Donor #36550) and 11 (Donor #8013L) days in culture. Samples were harvested by either papain [36] or oxalic acid digestion. Detailed methodology for papain and oxalic acid digestions are provided in Additional file 1.

Total DNA, sulfated glycosaminoglycan (s-GAG), and hydroxyproline content of papain digested lysates was quantified using the Hoechst dye 33258 assay [37], dimethylmethylene blue dye binding assay [38], and chloramine-T/Ehrlich's reagent assay [39], respectively. The insoluble elastin content of oxalic acid digested samples was measured using the Fastin™ Elastin Assay Kit by Biorcolor (Accurate Chemical and Scientific Corporation, cat. #CLRF2000). Additional details on biochemical assays are provided in Additional file 1.

### Fabrication and characterization of electrospun PCNU constructs

Polycarbonate polyurethane (PCNU) was synthesized as previously described [40]. Briefly, the base PCNU was synthesized from the reaction of poly(1,6-hexyl 1,2-ethyl carbonate)diol, 1,6-hexane diisocyanate, and 1,4-butanediol in N,N-dimethylacetamide at a molar ratio of 3:2:1, under an inert atmosphere of nitrogen. The polystyrene equivalent weight average molecular weight was estimated between  $99 \times 10^3$  and  $105 \times 10^3$  g/mol by gel permeation chromatography. Anionic dihydroxyl oligomer (ADO) was added to PCNU at a concentration of 0.15% (w/w) and dissolved in 1,1,1,3,3,3-hexafluoro-2-propanol to produce an 18% (w/v) PCNU polymer solution. The solution was electrospun through an 18-gauge stainless steel needle at a flow rate of 0.5 mL/hr onto a rotating mandrel (1150 rpm), at a distance of 18 cm, and an applied voltage of 18 kV (+17 kV at the needle and -1 kV at mandrel) into nanofibrous PCNU scaffolds. Scaffolds were dried overnight in a vacuum oven at 45 °C.

To confine hUCPVCs to electrospun PCNU scaffolds for cell culture, circular discs were removed from one electrospun sheet using a biopsy punch. The PCNU discs were placed over the opening of a 200 μL microfuge tube which had been modified to form a culture vessel by cutting off the end of the tube and excising the inner aspect of the tube cap, as previously described [40, 41]. The scaffold was held in place between the rim of the cap and the inner wall of the microfuge tube. PCNU discs in culture vessels were placed in 24-well plates (1 construct/well) and sterilized with ethylene oxide. Due to spatial heterogeneity within one sheet, each isolated region was counted as an independent sample.

Cell-free sterilized PCNU discs were isolated from culture vessels for characterization by scanning electron microscopy ( $N=3$ ) and biaxial mechanical testing ( $N=3$ ). Scanning electron microscopy was used to visualize scaffold fibres. Scanning electron micrographs were imported into Image J software for analysis of fibre diameter and alignment using the Diameter J plugin. Square samples (4.5 mm × 4.5 mm) were isolated from PCNU discs using a specimen cutter and underwent displacement controlled equibiaxial force testing (Biotester 5000; CellScale, Waterloo, CAN) in a PBS bath at 37 °C. Samples were mounted to the mechanical system using a tine attachment system (Biorakes with 0.7 mm tine spacing, CellScale, Waterloo, CAN), and a biaxial tensile testing protocol previously described by Labrosse et al. [42] was used. Strain tracking was conducted in the Biotester 5000's LabJoy software, and a MATLAB code from Labrosse et al. [42] was used to generate Green strain and membrane tension outputs.

### hUCPVC culture on electrospun PCNU scaffolds in StemMACS™

Sterilized PCNU scaffolds in modified culture vessels were pre-coated with 50 μL 1 mg/mL human plasma derived fibronectin (Sigma, cat #FC010) at a coating density of 2.5 μg/cm<sup>2</sup> in PBS overnight at 4 °C. Fibronectin solution was subsequently aspirated and scaffolds were washed with pre-warmed PBS (with calcium and magnesium) (37 °C) prior to cell seeding. hUCPVCs from one donor (Donor #0917003) were seeded on PCNU scaffolds at a density of 50,000 cells/cm<sup>2</sup> with 50 μL StemMACS™ culture media in modified culture vessels. An additional 500 μL/well of culture media was added to the 24-well plates housing the modified culture vessels. Cell culture media was replaced every other day.

### Cell morphology on electrospun PCNU scaffolds in StemMACS™

After 14 and 21 days in culture, hUCPVC-seeded PCNU constructs ( $N=3$  per timepoint) were harvested for

assessment of cell morphology by staining with FITC-labelled phalloidin (Sigma, cat #P5282) F-actin and Hoechst 33342 (Sigma, cat #B2261) nuclear stains before imaging by confocal microscopy. Details of the staining protocol are provided in Additional file 1.

Confocal images collected from three different locations on each construct were imported into Image J software for analysis of F-actin alignment. Z-stacks from the three locations on each sample were stratified into two groups to illustrate hUCPVCs in direct contact with PCNU scaffold fibres (PCNU-contacting) and those that had grown on top of the PCNU-contacting cells (cell-contacting). F-actin fibre alignment was quantified using the Orientation J vector field plugin in Image J.

### ECM protein synthesis on electrospun PCNU scaffolds in StemMACS™

After 14 and 21 days in culture, hUCPVC-seeded PCNU constructs ( $N=3$  per timepoint) were harvested for digestion by papain (day 14 and 21) and oxalic acid (day 21). Cell-free PCNU constructs that were incubated in parallel with cell-seeded scaffolds were similarly digested

to serve as negative controls for subsequent analyses. DNA, hydroxyproline, s-GAG and  $\alpha$ -elastin content associated with the cell-seeded constructs was quantified using the biochemical assays described above. Detailed methodology of digestion protocols and biochemical assays are provided in Additional file 1.

To visualize ECM proteins, hUCPVC-seeded PCNU constructs were stained using Movat’s pentachrome. Briefly, samples were harvested on day 21 of culture, embedded in optimal cutting temperature (OCT) compound and snap-frozen using liquid nitrogen. OCT-embedded samples were cryosectioned (10  $\mu\text{m}$ ) and subsequently stained with Movat’s pentachrome. Stained sections were imaged on a brightfield microscope.

### Statistical analysis

Graphical visualization of data and statistical analysis were performed using GraphPad Prism 9. Statistical differences between conditions were assessed using either two-way analysis of variance (ANOVA) with Tukey’s multiple comparisons test or Student’s t-test.

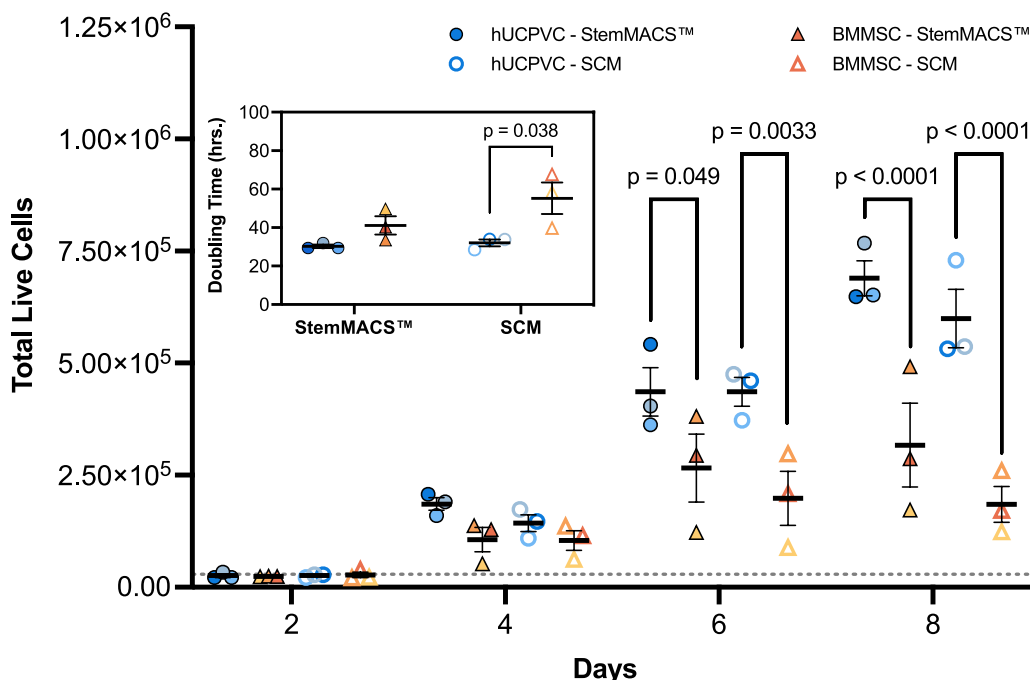


**Fig. 1** Proliferation and population doubling time of hUCPVCs ( $N=3$  donors,  $n=3$  technical replicates per donor) and BMMSCs ( $N=3$  donors,  $n=3$  technical replicates per donor) in xeno-free StemMACS™ and SCM. StemMACS™ culture medium supported the proliferation of both hUCPVCs and BMMSCs similarly to conventionally used SCM in an 8-day proliferation assay. Proliferation of hUCPVCs in each media formulation was similar to that of BMMSCs after 2 and 4 days in culture. After 6 and 8 days in culture, there were significantly more hUCPVCs than BMMSCs in both StemMACS™ (Day 6:  $p=0.049$ ; Day 8:  $p<0.0001$ ) and SCM (Day 6:  $p=0.0033$ ; Day 8:  $p<0.0001$ ) media conditions, suggesting a superior proliferative capacity of hUCPVCs. *Inset*: The average population doubling time of hUCPVCs was lower than that of their BMMSC counterparts in both StemMACS™ and SCM ( $p=0.038$ ), though this difference was only statistically significant in the latter media condition. Reported values are mean  $\pm$  SEM; statistical analysis by two-way ANOVA with post-hoc Tukey’s multiple comparisons test. Dashed grey line indicates initial cell seeding density in a 6-well plate. Each shade corresponds to a different donor of hUCPVCs (Donor 0917003; Donor 0917004; Donor 0317004 from dark to light shade of blue) and BMMSCs (Donor 8013L; Donor 36341; Donor 36550 from light to dark shade of yellow/orange)

All experimental data are presented as mean  $\pm$  standard error of the mean (SEM).

## Results

### Proliferation in StemMACS™

Proliferation of hUCPVCs and BMMSCs was compared in StemMACS™ culture medium and SCM. For both cell types, proliferation was similar in StemMACS™ versus SCM (Fig. 1). However, hUCPVCs proliferated more rapidly than BMMSCs in both StemMACS™ and SCM, with significantly more cells at day 6 ( $p < 0.05$ ) and day 8 ( $p < 0.0001$ ) (Fig. 1). Accordingly, the average population doubling time of hUCPVCs was shorter than that of BMMSCs in both StemMACS™ and SCM conditions, although this difference was only statistically significant in the SCM cohort ( $p = 0.038$ ) (Fig. 1, inset).

### Frequency of CFU-F in StemMACS™

The frequency of CFU-F in BMMSCs and hUCPVCs was assessed in StemMACS™ and SCM. BMMSCs had similar CFU-F frequencies (Fig. 2A) and colony size and density (Fig. 2B) in StemMACS™ medium and SCM. In contrast, hUCPVCs cultured in StemMACS™ had a significantly higher frequency of CFU-F than those in SCM ( $p = 0.012$ ) (Fig. 2A). Furthermore, hUCPVCs in StemMACS™ had notably larger and more densely populated colonies than their SCM cultured counterparts (Fig. 2B). No other conditions were statistically different, indicating that serum- and xeno-free StemMACS™ supported the clonal expansion of BMMSCs as well as SCM, while enhancing the clonal expansion of hUCPVCs compared to SCM.

### Osteogenic and adipogenic differentiation potential

All donors of BMMSCs demonstrated osteogenic differentiation potential as evidenced by positive alizarin red staining indicating calcium deposits (Fig. 3). Similarly, BMMSCs cultured in adipogenic media showed a capacity for adipogenesis as shown by positive oil red-O staining of lipid droplets (Fig. 3). When cultured in growth medium, BMMSCs did not differentiate to osteogenic or adipogenic lineages. hUCPVCs cultured in osteogenic induction media did not show evidence of differentiation after staining with alizarin red, similar to their growth medium cultured controls. Evidence of adipogenesis was also absent from hUCPVCs cultured in adipogenic culture medium and their growth medium cultured controls. Overall, after induction with the appropriate culture media, hUCPVCs did not demonstrate differentiation potential to either osteogenic or adipogenic lineages.

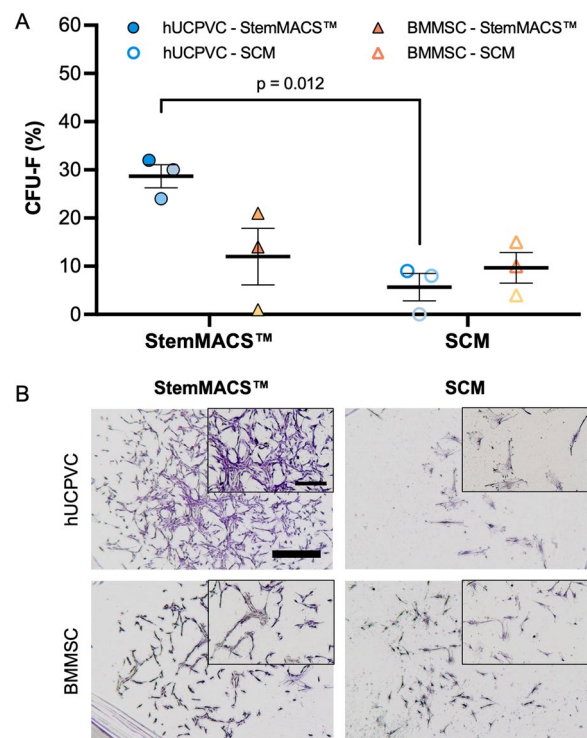


**Fig. 2** A Frequency of CFU-F in hUCPVCs and BMMSCs ( $N = 3$  donors each,  $n = 3$  technical replicates per donor) cultured in StemMACS™ and SCM. Culture with StemMACS™ resulted in a similar frequency of CFU-F compared to culture with SCM for BMMSCs. hUCPVCs cultured in StemMACS™ had a significantly higher frequency of CFU-F than their counterparts cultured in SCM ( $p = 0.012$ ). Reported values are mean  $\pm$  SEM; statistical analysis by two-way ANOVA with post-hoc Tukey's multiple comparisons test. Each shade corresponds to a different donor of hUCPVCs (Donor 0917003; Donor 0917004; Donor 0317004 from dark to light shade of blue) and BMMSCs (Donor 8013L; Donor 36341; Donor 36550 from light to dark shade of yellow/orange). B Crystal violet stained CFU-F colonies imaged under brightfield microscopy (scale bar = 1000  $\mu$ m; inset scale bar = 500  $\mu$ m). hUCPVCs cultured in StemMACS™ produced larger and more densely populated colonies than those cultured in SCM. BMMSCs consistently had smaller and less densely populated colonies than hUCPVCs in both media conditions

### ECM synthesis on tissue culture polystyrene in StemMACS™

Having established that StemMACS™ culture medium supported the proliferative capacity and CFU-F frequency of hUCPVCs and BMMSCs, we then investigated in vitro ECM synthesis by each cell type in serum- and xeno-free culture conditions. hUCPVC and BMMSCs were cultured in either StemMACS™ medium alone or StemMACS™ supplemented with 50  $\mu$ M AA for up to 14 days on tissue culture polystyrene (TCPS).

Total and DNA-normalized hydroxyproline (Fig. 4A, B),  $\alpha$ -elastin (Fig. 4C, D), and s-GAG content (Fig. 4E, F) were quantified in hUCPVC and BMMSC lysates via



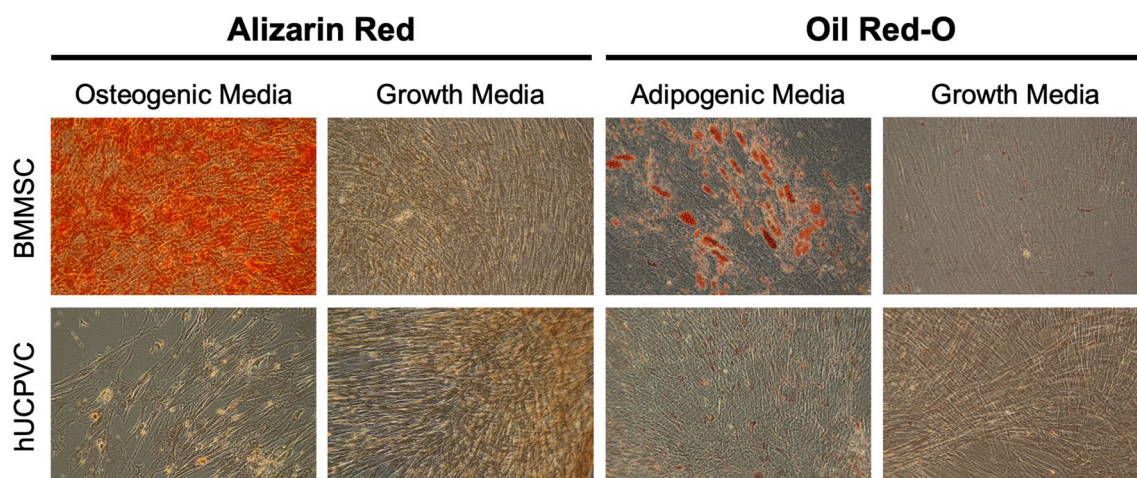


**Fig. 3** BMMSCs from all donors cultured in either osteogenic or adipogenic culture medium differentiated to osteogenic and adipogenic lineages as indicated by positive alizarin red and oil red-O staining, respectively. Conversely, none of the hUCPVC donors differentiated to either lineage. hUCPVC and BMMSC negative controls cultured in control SCM did not show differentiation to osteogenic or adipogenic lineages. Representative image from one biological donor shown for each cell type

biochemical analysis. hUCPVCs synthesized more total hydroxyproline than BMMSCs in StemMACS<sup>TM</sup> with or without AA supplementation, although this difference was only found to be statistically significant in unsupplemented StemMACS<sup>TM</sup> ( $p=0.021$ ) (Fig. 4A). hUCPVCs also synthesized more total  $\alpha$ -elastin than BMMSCs, in both unsupplemented ( $p=0.00026$ ) and AA-supplemented conditions ( $p<0.0001$ ) (Fig. 4C). Finally, total s-GAG synthesized by hUCPVCs was significantly greater than that synthesized by BMMSCs in both StemMACS<sup>TM</sup> ( $p=0.025$ ) and AA-supplemented StemMACS<sup>TM</sup> ( $p=0.049$ ) (Fig. 4E). Total DNA quantified in hUCPVC lysates was significantly greater than in BMMSCs in both StemMACS<sup>TM</sup> ( $p=0.0020$ ) and AA-supplemented StemMACS<sup>TM</sup> ( $p=0.0087$ ) (Fig. 4G).

When normalized to total DNA content, hUCPVCs deposited significantly more  $\alpha$ -elastin per unit DNA than BMMSCs with ( $p=0.042$ ) and without ( $p=0.035$ ) AA-supplementation (Fig. 4D). The DNA-normalized hydroxyproline (Fig. 4B) and s-GAG (Fig. 4F) content of hUCPVCs, though greater than that of their BMMSC

counterparts, were not significantly different in either basal or AA-supplemented StemMACS<sup>TM</sup>.

#### Culturing hUCPVCs on PCNU scaffolds in StemMACS<sup>TM</sup>— Cell morphology and ECM synthesis

Provided with evidence of the superior proliferative and ECM-synthesizing capacity of hUCPVCs over BMMSCs in StemMACS<sup>TM</sup> culture medium on TCPS, we then evaluated hUCPVCs as a prospective cell source for in vitro HVTE applications when cultured on a suitable biomaterial. hUCPVC were grown on electrospun nanofibrous PCNU scaffolds, a biodegradable biomaterial applicable to HVTE applications due to its highly aligned fibres and anisotropic mechanical behaviour (Fig. 5). After 14 and 21 days in culture, hUCPVC morphology on PCNU scaffolds was assessed by staining cytoskeletal F-actin. Confocal imaging revealed that hUCPVCs followed two principal directions of alignment based on proximity to the PCNU fibres. Cells in direct contact with scaffold

(See figure on next page.)

**Fig. 4** Quantification of total and DNA-normalized hydroxyproline (OH-proline) (A, B), elastin (C, D), and sulphated glycosaminoglycans (s-GAG) (E, F) synthesized by hUCPVCs and BMMSCs ( $N=3$  donors each,  $n=3$  technical replicates per donor) cultured in StemMACS<sup>TM</sup> and ascorbic acid (AA)-supplemented StemMACS<sup>TM</sup> culture media. hUCPVCs synthesized significantly more total A OH-proline ( $p=0.021$ ), C elastin ( $p=0.00026$ ) and E s-GAG ( $p=0.025$ ) than their BMMSC counterparts cultured in StemMACS<sup>TM</sup>. Supplementation with 50  $\mu$ M AA did not significantly alter ECM protein synthesis in either cell population. Similarly, DNA-normalized B OH-proline, D elastin, and F s-GAG content in hUCPVC cultures was higher than that of BMMSCs in both StemMACS<sup>TM</sup> and AA-supplemented StemMACS<sup>TM</sup> culture media, although this difference was only statistically significant for DNA-normalized elastin content ( $p=0.042$  and  $p=0.035$ , respectively). G Total DNA content of hUCPVCs cultured in StemMACS<sup>TM</sup> and AA-supplemented StemMACS<sup>TM</sup> culture media was significantly greater than that of their BMMSC counterparts ( $p=0.0020$  and  $p=0.0087$ ). Reported values are mean  $\pm$  SEM; statistical analysis by unpaired t-test. Each shade corresponds to a different donor of hUCPVCs (Donor 0917003; Donor 0917004; Donor 0317004 from dark to light shade of blue) and BMMSCs (Donor 8013L; Donor 36341; Donor 36550 from light to dark shade of yellow/orange)



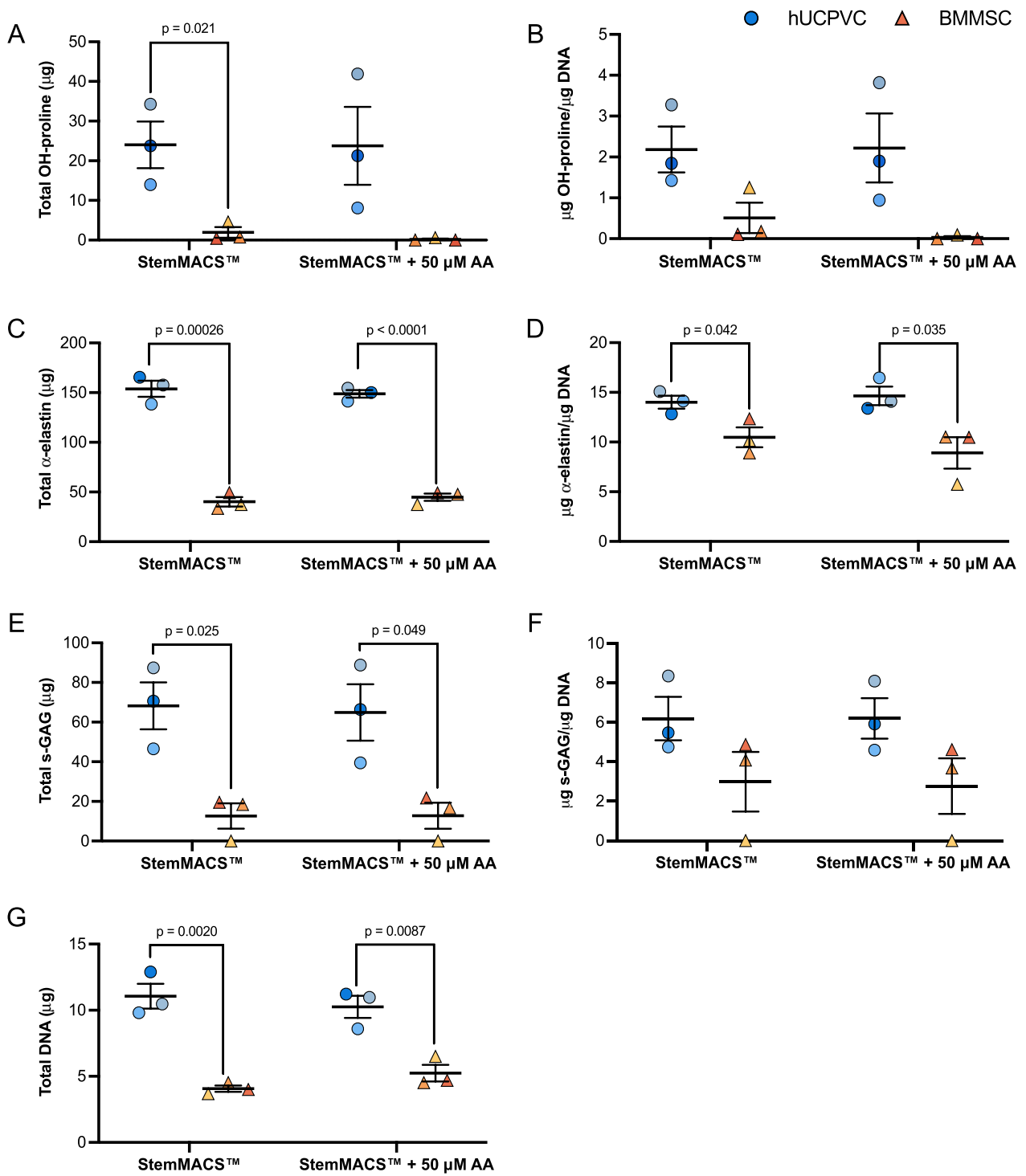


**Fig. 4** (See legend on previous page.)

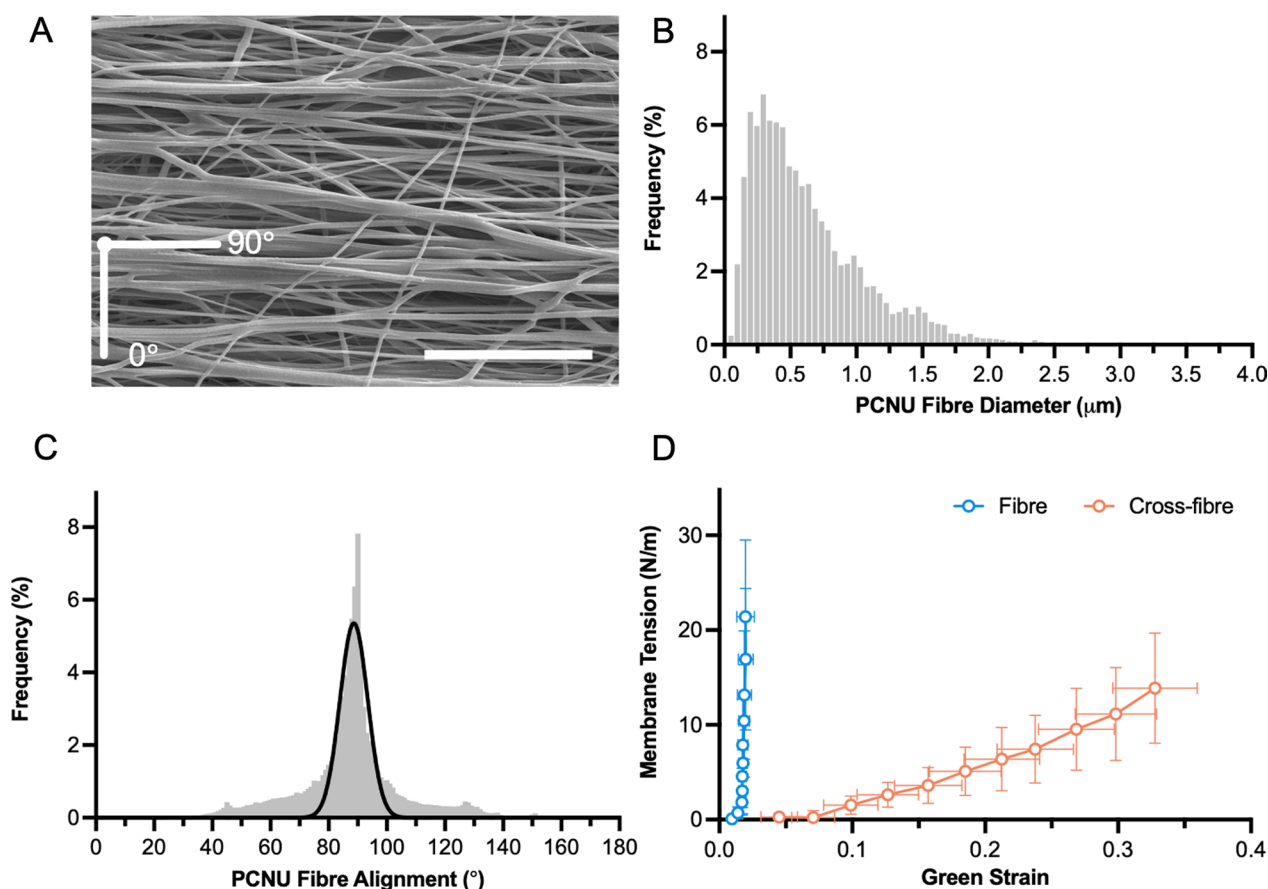


**Fig. 5** Characterization of PCNU scaffolds by scanning electron microscopy and biaxial tensile testing. **A** Representative scanning electron microscopy image of PCNU fibres in an electrospun biomaterial sheet (scale bar = 20 μm). Three separate regions of the electrospun sheet were isolated for scanning electron microscopy imaging and subsequent quantification of fibre diameter and orientation, and biaxial mechanical properties ( $N=3$ ). **B** Electrospun PCNU fibres were  $447 \pm 56.7$  nm (mean  $\pm$  SD) in diameter and **C** followed a principal direction of alignment, that conferred **D** anisotropic tensile properties to the PCNU scaffolds with greater compliance in the cross-fibre direction than the fibre direction

fibres showed a high degree of alignment with PCNU fibres ( $90^\circ$ ) on days 14 ( $88.62^\circ \pm 10.47^\circ$ ) and 21 ( $88.79^\circ \pm 14.02^\circ$ ) (Fig. 6). Moving away from the surface of the PCNU scaffolds, where cells were layered on top of other cells and not in direct contact with the fibres, the direction of hUCPVC alignment shifted away from that of the PCNU fibres (Fig. 6).

Quantification of ECM deposition after 14 and 21 days of culture on PCNU scaffolds revealed that hUCPVCs retained their capacity to synthesize hydroxyproline (Fig. 7A, B),  $\alpha$ -elastin (Fig. 7C, D) and s-GAG (Fig. 7E, F). When normalized to DNA amount, the hydroxyproline content of hUCPVC-seeded constructs was similar to that on TCPS (Fig. 7B vs Fig. 4B), while DNA-normalized  $\alpha$ -elastin content was approaching the levels synthesized on TCPS (Fig. 7D vs Fig. 4D). By contrast, DNA-normalized s-GAG content was approximately 2.5 fold greater on PCNU than TCPS (Fig. 7F vs Fig. 4F). Finally, evaluation of the spatial distribution of hUCPVCs cultured

on PCNU scaffolds by Movat's pentachrome staining revealed multiple cell and tissue layers growing atop the PCNU scaffold (Fig. 7F).

## Discussion

Despite their convenience to autologous HVTE for pediatric CHDs [24, 25, 27–30], umbilical cord-derived MSCs are understudied in this context. In particular, hUCPVCs derived explicitly from the cell and ECM rich perivascular sub-region of the cord's WJ have not been exploited for their utility to pediatric HVTE applications. This knowledge gap is widened by the absence of literature evaluating ECM synthesis under serum- and xeno-free conditions by hUCPVCs for the purpose of HVTE. Here we demonstrated for the first time that hUCPVCs can be successfully grown in serum- and xeno-free culture

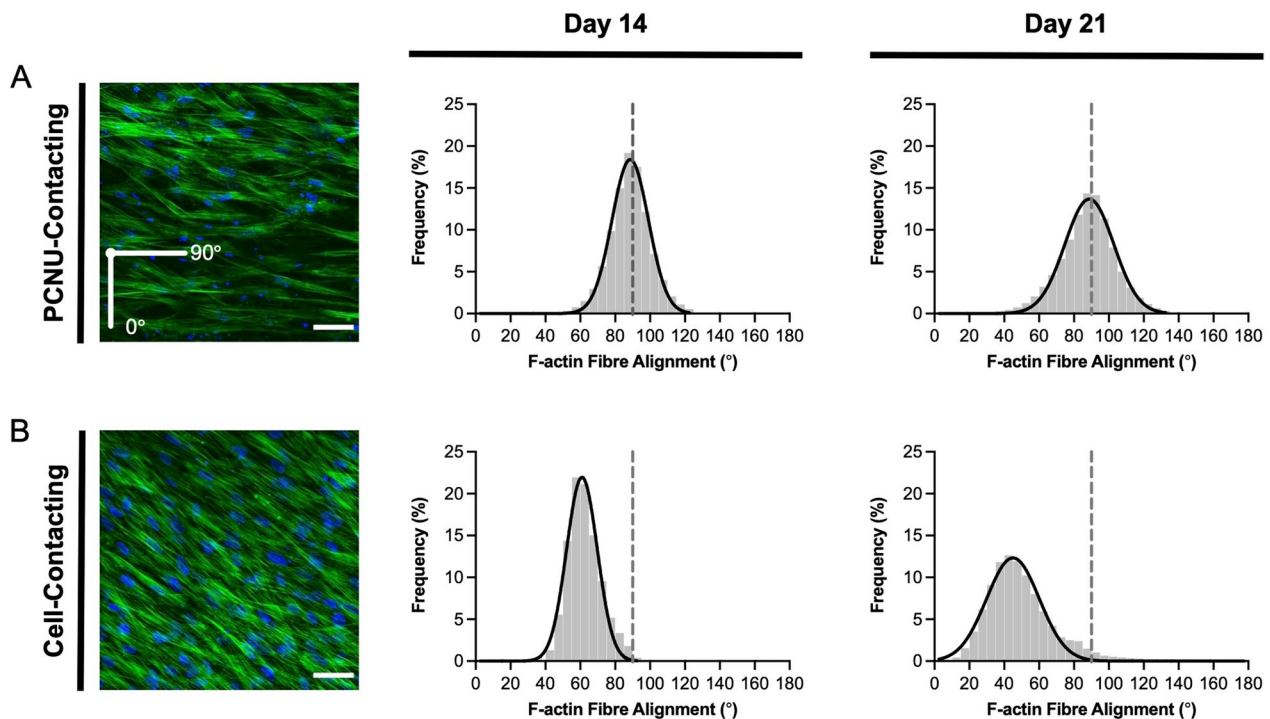


**Fig. 6** F-actin (green) and nuclear (blue) staining of hUCPVCs cultured on electrospun PCNU for 14 and 21 days in StemMACS™. Confocal images and frequency distribution plot of F-actin alignment in hUCPVC-seeded PCNU scaffolds ( $N = 3$ ) showed two principal angles of cell alignment: **A** hUCPVCs in direct contact with PCNU fibres aligned with the scaffold fibres ( $90^\circ$ ), whereas **B** hUCPVCs growing on a monolayer of cells away from the surface of the scaffold aligned away from the principal direction of the PCNU fibres. PCNU fibres oriented at  $90^\circ$  marked by a grey dashed line on frequency distribution plots. Confocal images of hUCPVC-seeded PCNU constructs are representative of  $N = 3$  on day 14 (scale bar =  $50 \mu\text{m}$ )

media to synthesize the constituent ECM proteins of the native valve *in vitro*, incentivizing their use for the clinical realization of autologous pediatric TEHVs.

Clinical translation of *in vitro* TEHVs will ultimately require adherence to GMP guidelines to yield a reproducible construct. The inherent lot-to-lot variability and undefined composition of FBS motivate early adoption of serum- and xeno-free culture of candidate cells in regenerative studies as an important step in the realization of protocols that align with GMP guidelines. The first objective of our study was to determine whether a commercially available serum- and xeno-free culture medium, StemMACS™, was comparable to conventionally used SCM in its capacity to support the proliferative and clonogenic potential of hUCPVCs and BMMSCs. We found that both hUCPVCs and BMMSCs cultured in StemMACS™ media proliferated as well as their SCM cultured counterparts. This is consistent with the findings of other groups that showed umbilical cord MSCs [43–48] and BMMSCs [49] exhibit similar or improved proliferation

in serum- and xeno-free conditions over SCM. We also demonstrated that serum-free culture conferred greater clonogenic potential to hUCPVCs over SCM, which is consistent with previous studies on WJ MSCs in serum-free and serum-containing conditions [43–48]. Two notable exceptions to our findings and those of previous studies come from Wang et al. [50] and Chen et al. [51], wherein the proliferative capacity of umbilical cord MSCs was greater in SCM. Unlike what was observed for hUCPVCs, we did not find that the colony forming capacity of BMMSCs differed between StemMACS™ and SCM. The measured CFU-F frequency of BMMSCs in SCM was similar to that reported by Bhat et al., although they reported a significant decrease in clonogenicity in StemMACS™, when compared to SCM [49]. Nevertheless, our findings largely affirm trends reported in the literature, which overwhelmingly favour serum- and xeno-free culture for both umbilical cord MSCs and BMMSCs.



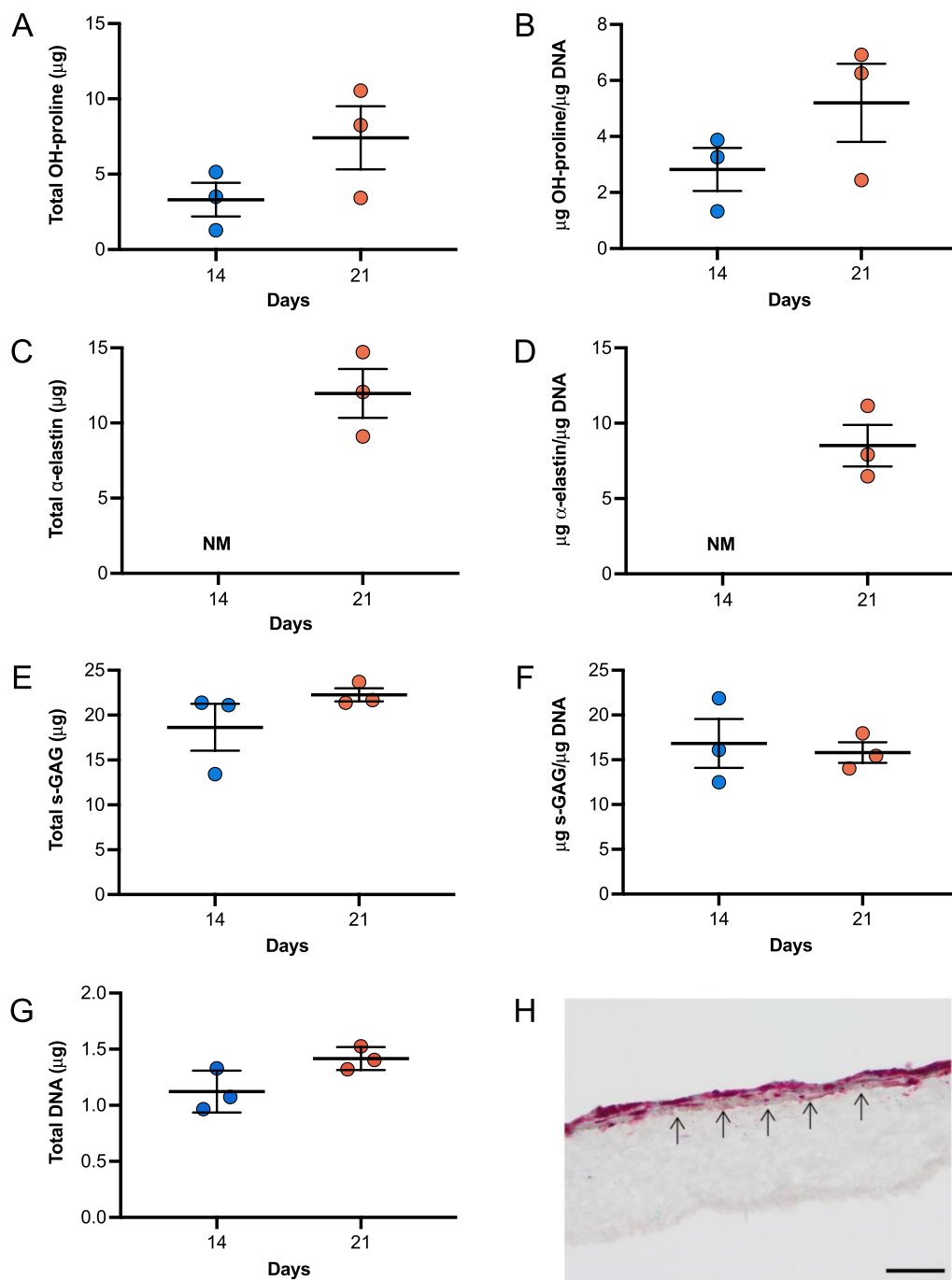


**Fig. 7** Quantification of total and DNA-normalized hydroxyproline (OH-proline) (**A–B**), elastin (**C–D**), and sulphated glycosaminoglycans (s-GAG) (**E–F**) synthesized by hUCPVCs from a single donor cultured on electrospun PCNU ( $N=3$ ) for 14 and 21 days in StemMACS™ culture medium. Total **A** OH-proline, **E** s-GAG and **G** DNA content increased between 14 and 21 days in culture, although this change was not statistically significant. Elastin deposition after 14 days of culture was not measured (NM) and time-dependent changes in elastin content were not evaluated. DNA-normalized **B** OH-proline and **D** elastin content was similar to or approaching that on tissue culture polystyrene (Fig. 4B and D), while DNA-normalized s-GAG content was greater than in tissue culture polystyrene (Fig. 4F). **H** Movat's pentachrome staining of hUCPVC-seeded PCNU constructs shows that the cells and deposited ECM grew in layers above the PCNU scaffold. Black arrows label boundary between hUCPVC and scaffold (scale bar = 50 µm). Reported values are mean ± SEM; statistical analysis by unpaired t-test

A direct comparison of the two cell populations in each culture condition showed that hUCPVCs proliferated more than their BMMSC counterparts, as evidenced by significantly higher cell counts and shorter population doubling times. Moreover, hUCPVCs had greater clonogenic potential than BMMSCs in StemMACS™. The superior proliferative and colony forming capacity of hUCPVCs over BMMSCs can be a result of different factors. First, BMMSCs experienced contact-inhibited growth after a confluent monolayer was produced, whereas hUCPVCs continued to grow in multiple layers (data not shown). This phenomenon was previously reported by Baksh et al. in SCM [19] and reinforced by a recent report from Bhat et al. that found cumulative population doublings decreased as a function of higher cell-seeding density of BMMSCs in both SCM and StemMACS™ [49]. Secondly, MSCs derived from adult tissue sources reach replicative senescence at lower passages than MSCs harvested from fetal or neonatal sources [52]. All experiments in this study were conducted with neonatal hUCPVCs at passage 3 and adult BMMSCs at passage 4 or 5. hUCPVCs have been reported to have a consistent CFU-F frequency over 10 passages in SCM [22]. Furthermore, studies of WJ MSCs revealed that a negligible proportion of senescent cells could be detected in serum and xeno-free media, whereas nearly 30% of WJ MSCs in SCM were senescent [43]. Previous findings suggest that replicative senescence of umbilical cord MSCs is either not detectable or delayed to late passages (>10) [21, 50], whereas adult BMMSCs can undergo senescence as early as passage 7 [52].

In this study we found an absence of osteogenic and adipogenic differentiation potential among all hUCPVC donors. Previous studies on hUCPVCs [19], umbilical cord MSCs [21, 43–47, 50] and BMMSCs [46] have demonstrated that osteogenic and adipogenic differentiation potential of cells are retained regardless of whether the cells are isolated in SCM or serum- and xeno-free culture media. However, some groups have shown that compared to MSCs sourced from adult tissues, the adipogenic differentiation potential of neonatal hUCPVCs and WJ MSCs is significantly dampened as a result of delayed and reduced activation of the PPAR $\gamma$  transcription factor cascade [53], which is deemed essential to adipogenic differentiation. In the context of HVTE, the lack of osteogenic and adipogenic differentiation potential of hUCPVCs is favourable given that these lineages are associated with native valve pathology [54]. It should, however, be noted that the absence of osteogenic and adipogenic differentiation of hUCPVCs in vitro cannot predict how the cells will behave in situ.

The second objective of this study was to evaluate the capacity of StemMACS™ cultured hUCPVCs and

BMMSCs to synthesize ECM proteins in vitro. The ECM proteins of the native PV - collagen, s-GAG, and elastin - are critical to its structure and function. Thus, in vitro HVTE strategies rely on MSCs to synthesize and organize the three constituent proteins of the ECM. We found that hUCPVCs deposited significantly more total collagen, s-GAG, and elastin than BMMSCs when cultured in StemMACS™. Cultures are often supplemented with AA to increase cell proliferation and collagen, s-GAG, and elastin deposition in a dose-dependent manner [55]. Here, we found no effect of AA supplementation of StemMACS™ on total DNA or ECM content, in either hUCPVCs or BMMSCs. It is likely that the proprietary StemMACS™ formulation itself contains AA and the cell response is saturated, rendering further supplementation with AA either inconsequential or pessimal to ECM synthesis. We can only speculate on this issue as the use of a commercial media with a proprietary formulation does not allow us to attribute the observed benefits to a single or specific combination of components. The greater total ECM synthesis capacity of hUCPVCs likely stems from its superior proliferative capacity over BMMSCs, as DNA-normalized collagen and s-GAG content, though greater than that of BMMSCs, was not found to be significantly different, whereas, the total cellularity and ECM protein content of hUCPVC cultures was significantly greater than BMMSCs. While the results of our studies favour the use of hUCPVCs over BMMSCs for in vitro HVTE, future works should also include hUCPVCs sourced from female donors to account for any sex-dependent differences in cell behaviour.

In a further assessment of their candidacy for in vitro HVTE, we cultured hUCPVCs on electrospun nanofibrous PCNU scaffolds with aligned fibres in StemMACS™. hUCPVCs retained their capacity to synthesize collagen, s-GAG, and elastin on nanofibrous PCNU. The DNA-normalized collagen, expressed as hydroxyproline, and s-GAG deposition reported here exceeded the maximum values reported previously for umbilical cord MSCs cultured on a synthetic scaffold to produce a living patch [24] and valved conduit [25]. The superior synthetic capacity of hUCPVCs in StemMACS™ under static conditions is notable, as these previous studies required SCM and mechanical conditioning of the engineered tissues in bioreactors to maximize ECM synthesis [24, 25]. Also favourable was that hUCPVCs adjacent to the scaffold aligned with the PCNU fibres. Aligned fibrous scaffolds are desirable for HVTE as they confer anisotropic tensile properties analogous to the native PV [56] and can direct cell and ECM alignment with the principal direction of the fibres [57] in order to mimic the orientation of

collagen and elastin fibres in the native valve [58]. The off-axis alignment of cells in tissue layers away from the scaffold was ostensibly because of loss of contact guidance from the scaffold. This could be mitigated in the future by increasing the porosity of the scaffold to facilitate greater tissue infiltration amongst the fibres [59, 60] or by mechanical conditioning in a strain bioreactor [61], a strategy that has been shown to enhance cell and ECM alignment [62].

## Conclusion

Serum- and xeno-free StemMACS™ medium supported culture of both hUCPVCs and BMMSCs, but hUCPVCs demonstrated superior proliferative, clonogenic, and ECM synthesizing capacity in vitro. Similarly, hUCPVCs cultured in StemMACS™ media on electrospun PCNU valve tissue engineering scaffolds deposited tissue containing collagen, s-GAG and elastin on the scaffold surface, where they aligned with the scaffold fibres. Together, these findings support hUCPVCs as a promising autologous cell source for in vitro HVTE to address the clinical need in pediatric patients with CHD.

## Abbreviations

AA	Ascorbic acid
ADO	Anionic dihydroxyl oligomer
ANOVA	Analysis of variance
BMMSC	Bone marrow-derived MSC
CFU-F	Colony forming unit-fibroblasts
CHD	Congenital heart defect
ECM	Extracellular matrix
GMP	Good manufacturing practices
hUCPVC	Human umbilical cord perivascular cell
HVTE	Heart valve tissue engineering
ISCT	International Society for Cell and Gene Therapy
MSC	Mesenchymal stromal cell
OCT	Optimal cutting temperature
PBS	Phosphate buffered saline
PCNU	Polycarbonate polyurethane
SCM	Serum-containing media
s-GAG	Sulfated glycosaminoglycan
TEHV	Tissue engineered heart valve
SEM	Standard error of the mean

## Supplementary Information

The online version contains supplementary material available at <https://doi.org/10.1186/s13287-023-03318-3>.

**Additional file 1.** Supplemental Materials and Methods.

## Acknowledgements

The authors thank Tissue Regeneration Therapeutics, Inc. (Toronto, ON) for providing human umbilical cord perivascular cells for this study. The authors thank Edwin Wong and Dr. Henrik Persson for their feedback on the analysis of confocal images.

## Author contributions

SPN: Conception and design, collection and assembly of data, data analysis and interpretation, manuscript writing, final approval of manuscript. ML: Collection of data (confocal imaging, scanning electron microscopy imaging and

analysis), final approval of manuscript. BM: Collection of data (mechanical testing and analysis), final approval of manuscript. NMS: Provision of study materials (synthesis of PCNU polymer), final approval of manuscript. ZM: Collection of data (histology), final approval of manuscript. JPS: Provision of study materials (PCNU polymer), administrative support, final approval of manuscript. JED: Provision of study materials (hUCPVCs), administrative support, final approval of manuscript. CAS: Conception and design, financial support, provision of study materials, manuscript writing, final approval of manuscript. All authors read and approved the final manuscript.

## Funding

This work was supported by a grant from the Canadian Institute of Health Research/National Sciences and Engineering Research Council Collaborative Health Research Project (CPG-151962/CHRPJ/CHRPJ 508364–17) and seed funding from the Translational Biology and Engineering Program in the Ted Rogers Centre for Heart Research. The authors are grateful to the del Moral family for their support of this study.

## Availability of data and materials

The data that support the findings of this study are available from the corresponding author upon reasonable request.

## Declarations

### Ethics approval and consent to participate

BMMSCs were provided under a material transfer agreement with the Texas A&M Health Science Centre College of Medicine Institute for Regenerative Medicine at Scott & White. hUCPVCs were provided in-kind to the authors by Tissue Regeneration Therapeutics. Ethics approval and consent to participate for procurement of the cells were obtained by the providers of the cells in adherence with the Declaration of Helsinki.

### Consent for publication

Not applicable.

### Competing interests

Dr. John E. Davies is the founding President and CEO of Tissue Regeneration Therapeutics, Inc. (Toronto, ON) who provided the human umbilical cord perivascular cells used in this study. The other authors declare no conflicts of interest.

### Author details

<sup>1</sup>Translational Biology and Engineering Program, Ted Rogers Centre for Heart Research, Toronto, Canada. <sup>2</sup>Institute of Biomedical Engineering, University of Toronto, Toronto, Canada. <sup>3</sup>Department of Mechanical and Industrial Engineering, University of Toronto, Toronto, Canada. <sup>4</sup>Faculty of Dentistry, University of Toronto, Toronto, Canada. <sup>5</sup>Tissue Regeneration Therapeutics, Toronto, Canada.

Received: 30 October 2022 Accepted: 29 March 2023

Published online: 19 April 2023

## References

- Bacha E. Valve-sparing or valve reconstruction options in tetralogy of fallot surgery. *Semin Thorac Cardiovasc Surg Pediatr Cardiac Surg Ann.* 2017;20:79–83.
- Patukale A, Daley M, Betts K, Justo R, Dhannapuneni R, Venugopal P, et al. Outcomes of pulmonary valve leaflet augmentation for transannular repair of tetralogy of Fallot. *J Thorac Cardiovasc Surg.* 2021;162(5):1313–20.
- Fioretta ES, Motta SE, Lintas V, Loerakker S, Parker KK, Baaijens FPT, et al. Next-generation tissue-engineered heart valves with repair, remodelling and regeneration capacity. *Nat Rev Cardiol.* 2020;18(2):92–116.
- Mirani B, Parvin Nejad S, Simmons CA. Recent progress toward clinical translation of tissue-engineered heart valves. *Can J Cardiol.* 2021;37(7):1064–77.



5. Liu AC, Joag VR, Gottlieb AI. The emerging role of valve interstitial cell phenotypes in regulating heart valve pathobiology. *Am J Pathol*. 2007;171(5):1407–18.
6. Schmidt D, Dijkman PE, Driessen-Mol A, Stenger R, Mariani C, Puolakka A, et al. Minimally-invasive implantation of living tissue engineered heart valves: a comprehensive approach from autologous vascular cells to stem cells. *J Am Coll Cardiol*. 2010;56(6):510–20.
7. Emmert MY, Schmitt BA, Loerakker S, Sanders B, Spriestersbach H, Fioretta ES, et al. Computational modeling guides tissue-engineered heart valve design for long-term in vivo performance in a translational sheep model. *Sci Transl Med*. 2018;10(440):eaan4587.
8. Motta SE, Fioretta ES, Dijkman PE, Lintas V, Behr L, Hoerstrup SP, et al. Development of an off-the-shelf tissue-engineered sinus valve for transcatheter pulmonary valve replacement: a proof-of-concept study. *J Cardiovasc Transl Res*. 2018;11(3):182–91.
9. Fioretta ES, Lintas V, Mallone A, Motta SE, von Boehmer L, Dijkman PE, et al. Differential leaflet remodeling of bone marrow cell pre-seeded versus nonseeded bioresorbable transcatheter pulmonary valve replacements. *JACC Basic Transl Sci*. 2020;5(1):15–31.
10. Berglund AK, Fortier LA, Antczak DF, Schnabel LV. Immunoprivileged no more: measuring the immunogenicity of allogeneic adult mesenchymal stem cells. *Stem Cell Res Ther*. 2017;8(1):288.
11. Rowland AL, Miller D, Berglund A, Schnabel LV, Levine GJ, Antczak DF, et al. Cross-matching of allogeneic mesenchymal stromal cells eliminates recipient immune targeting. *Stem Cells Transl Med*. 2021;10(5):694–710.
12. Schmidt D, Achermann J, Odermatt B, Breyman C, Mol A, Genoni M, et al. Prenatally fabricated autologous human living heart valves based on amniotic fluid derived progenitor cells as single cell source. *Circulation*. 2007;116(11 Suppl):164–70.
13. Schmidt D, Hoerstrup SP. Tissue engineered heart valves based on human cells. *Swiss Med Wkly*. 2007;137(Suppl 155):s80s–s85.
14. Petsche Connell J, Camci-Unal G, Khademhosseini A, Jacot JG. Amniotic fluid-derived stem cells for cardiovascular tissue engineering applications. *Tissue Eng Part B Rev*. 2013;19(4):368–79.
15. Weiss ML, Troyer DL. Stem cells in the umbilical cord. *Stem cell Rev*. 2006;2(2):155–62.
16. Sarugaser R, Lickorish D, Baksh D, Hosseini MM, Davies JE. Human umbilical cord perivascular (HUCPV) cells: a source of mesenchymal progenitors. *Stem cells (Dayton, Ohio)*. 2005;23(2):220–9.
17. Conconi MT, Burra P, Di Liddo R, Calore C, Turetta M, Bellini S, et al. CD105(+) cells from Wharton's jelly show in vitro and in vivo myogenic differentiation potential. *Int J Mol Med*. 2006;18(6):1089–96.
18. Dominici M, Lelanc K, Mueller I, Slaper-Cortenbach I, Marini F, Krause D, et al. Minimal criteria for defining multipotent mesenchymal stromal cells. *Int Soc Cell Ther Position Statement Cytotherapy*. 2006;8(4):315–7.
19. Baksh D, Yao R, Tuan RS. Comparison of proliferative and multilineage differentiation potential of human mesenchymal stem cells derived from umbilical cord and bone marrow. *Stem cells (Dayton, Ohio)*. 2007;25(6):1384–92.
20. Sarugaser R, Ennis J, Stanford WL, Davies JE. Isolation, propagation, and characterization of human umbilical cord perivascular cells (HUCPVCs). *Methods Mol Biol (Clifton, NJ)*. 2009;482:269–79.
21. Subramanian A, Fong CY, Biswas A, Bongso A. Comparative characterization of cells from the various compartments of the human umbilical cord shows that the Wharton's jelly compartment provides the best source of clinically utilizable mesenchymal stem cells. *PLoS ONE*. 2015;10(6): e0127992.
22. Sarugaser R, Hanoun L, Keating A, Stanford WL, Davies JE. Human mesenchymal stem cells self-renew and differentiate according to a deterministic hierarchy. *PLoS ONE*. 2009;4(8): e6498.
23. Zebardast N, Lickorish D, Davies JE. Human umbilical cord perivascular cells (HUCPVC): A mesenchymal cell source for dermal wound healing. *Organogenesis*. 2010;6(4):197–203.
24. Schmidt D, Mol A, Neuenschwander S, Breyman C, Gossi M, Zund G, et al. Living patches engineered from human umbilical cord derived fibroblasts and endothelial progenitor cells. *Eur J Cardio-Thorac Surg Off J Eur Assoc Cardio-Thorac Surg*. 2005;27(5):795–800.
25. Schmidt D, Mol A, Odermatt B, Neuenschwander S, Breyman C, Gossi M, et al. Engineering of biologically active living heart valve leaflets using human umbilical cord-derived progenitor cells. *Tissue Eng*. 2006;12(11):3223–32.
26. Iacobazzi D, Rapetto F, Albertario A, Swim MM, Narayan S, Skeffington K, et al. Wharton's jelly-mesenchymal stem cell-engineered conduit for pediatric translation in heart defect. *Tissue Eng Part A*. 2021;27(3–4):201–13.
27. Schmidt D, Asmis LM, Odermatt B, Kelm J, Breyman C, Gossi M, et al. Engineered living blood vessels: functional endothelia generated from human umbilical cord-derived progenitors. *Ann Thorac Surg*. 2006;82(4):1465–71.
28. Kadner A, Hoerstrup SP, Tracy J, Breyman C, Maurus CF, Melnitchouk S, et al. Human umbilical cord cells: a new cell source for cardiovascular tissue engineering. *Ann Thorac Surg*. 2002;74(4):S1422–8.
29. Hoerstrup SP, Kadner A, Breyman C, Maurus CF, Guenter CI, Sodan R, et al. Living, autologous pulmonary artery conduits tissue engineered from human umbilical cord cells. *Ann Thorac Surg*. 2002;74(1):46–52.
30. Kadner A, Zund G, Maurus C, Breyman C, Yakarisik S, Kadner G, et al. Human umbilical cord cells for cardiovascular tissue engineering: a comparative study. *Eur J Cardio Thorac Surg Off J Eur Assoc Cardio Thorac Surg*. 2004;25(4):635–41.
31. Hawkes PW. Fetal bovine serum: geographic origin and regulatory relevance of viral contamination. *Bioresour Bioprocess*. 2015;2(1):34.
32. Pilgrim CR, McCahill KA, Rops JG, Dufour JM, Russell KA, Koch TG. A review of fetal bovine serum in the culture of mesenchymal stromal cells and potential alternatives for veterinary medicine. *Front Vet Sci*. 2022;9: 859025.
33. Spees JL, Gregory CA, Singh H, Tucker HA, Peister A, Lynch PJ, et al. Internalized antigens must be removed to prepare hypoimmunogenic mesenchymal stem cells for cell and gene therapy. *Mol Ther*. 2004;9(5):747–56.
34. Khodabukus A, Baar K. The effect of serum origin on tissue engineered skeletal muscle function. *J Cell Biochem*. 2014;115(12):2198–207.
35. Baker M. Reproducibility: respect your cells! *Nature*. 2016;537(7620):433–5.
36. Hoemann CD. Molecular and biochemical assays of cartilage components. *Methods Mol Med*. 2004;101:127–56.
37. Kim YJ, Sah RL, Doong JY, Grodzinsky AJ. Fluorometric assay of DNA in cartilage explants using Hoechst 33258. *Anal Biochem*. 1988;174(1):168–76.
38. Farnedale RW, Sayers CA, Barrett AJ. A direct spectrophotometric microassay for sulfated glycosaminoglycans in cartilage cultures. *Connect Tissue Res*. 1982;9(4):247–8.
39. Woessner JF Jr. The determination of hydroxyproline in tissue and protein samples containing small proportions of this imino acid. *Arch Biochem Biophys*. 1961;93:440–7.
40. Yang L, Kandel RA, Chang G, Santerre JP. Polar surface chemistry of nanofibrous polyurethane scaffold affects annulus fibrosus cell attachment and early matrix accumulation. *J Biomed Mater Res Part A*. 2009;91(4):1089–99.
41. Attia M, Santerre JP, Kandel RA. The response of annulus fibrosus cell to fibronectin-coated nanofibrous polyurethane-anionic dihydroxyoligomer scaffolds. *Biomaterials*. 2011;32(2):450–60.
42. Labrosse MR, Jafar R, Ngu J, Boodhwani M. Planar biaxial testing of heart valve cusp replacement biomaterials: experiments, theory and material constants. *Acta Biomater*. 2016;45:303–20.
43. Swamynathan P, Venugopal P, Kannan S, Thej C, Kolkundar U, Bhagwat S, et al. Are serum-free and xeno-free culture conditions ideal for large scale clinical grade expansion of Wharton's jelly derived mesenchymal stem cells? a comparative study. *Stem Cell Res Ther*. 2014;5(4):88.
44. Wu X, Kang H, Liu X, Gao J, Zhao K, Ma Z. Serum and xeno-free, chemically defined, no-plate-coating-based culture system for mesenchymal stromal cells from the umbilical cord. *Cell Prolif*. 2016;49(5):579–88.
45. Wu M, Han ZB, Liu JF, Wang YW, Zhang JZ, Li CT, et al. Serum-free media and the immunoregulatory properties of mesenchymal stem cells in vivo and in vitro. *Cell Physiol Biochem Int J Exp Cell Physiol Biochem Pharmacol*. 2014;33(3):569–80.
46. Simoes IN, Boura JS, dos Santos F, Andrade PZ, Cardoso CM, Gimble JM, et al. Human mesenchymal stem cells from the umbilical cord matrix: successful isolation and ex vivo expansion using serum-/xeno-free culture media. *Biotechnol J*. 2013;8(4):448–58.
47. Hartmann I, Hollweck T, Haffner S, Krebs M, Meiser B, Reichart B, et al. Umbilical cord tissue-derived mesenchymal stem cells grow best under

- GMP-compliant culture conditions and maintain their phenotypic and functional properties. *J Immunol Methods*. 2010;363(1):80–9.
48. Le HM, Nguyen LT, Hoang DH, Bach TQ, Nguyen HTN, Mai HT, et al. Differential development of umbilical cord-derived mesenchymal stem cells during long-term maintenance in fetal bovine serum-supplemented medium and xeno- and serum-free culture medium. *Cell Reprogram*. 2021;23(6):359–69.
  49. Bhat S, Viswanathan P, Chandanala S, Prasanna SJ, Seetharam RN. Expansion and characterization of bone marrow derived human mesenchymal stromal cells in serum-free conditions. *Sci Rep*. 2021;11(1):3403.
  50. Wang Y, Wu H, Yang Z, Chi Y, Meng L, Mao A, et al. Human mesenchymal stem cells possess different biological characteristics but do not change their therapeutic potential when cultured in serum free medium. *Stem Cell Res Ther*. 2014;5(6):132.
  51. Chen G, Yue A, Ruan Z, Yin Y, Wang R, Ren Y, et al. Human umbilical cord-derived mesenchymal stem cells do not undergo malignant transformation during long-term culturing in serum-free medium. *PLoS ONE*. 2014;9(6): e98565.
  52. Hass R, Kasper C, Böhm S, Jacobs R. Different populations and sources of human mesenchymal stem cells (MSC): a comparison of adult and neonatal tissue-derived MSC. *Cell Commun Signal*. 2011;9:12.
  53. Ragni E, Viganò M, Parazzi V, Montemurro T, Montelatici E, Lavazza C, et al. Adipogenic potential in human mesenchymal stem cells strictly depends on adult or foetal tissue harvest. *Int J Biochem Cell Biol*. 2013;45(11):2456–66.
  54. Chen JH, Yip CY, Sone ED, Simmons CA. Identification and characterization of aortic valve mesenchymal progenitor cells with robust osteogenic calcification potential. *Am J Pathol*. 2009;174(3):1109–19.
  55. Choi KM, Seo YK, Yoon HH, Song KY, Kwon SY, Lee HS, et al. Effect of ascorbic acid on bone marrow-derived mesenchymal stem cell proliferation and differentiation. *J Biosci Bioeng*. 2008;105(6):586–94.
  56. van Geemen D, Soares AL, Oomen PJ, Driessen-Mol A, Janssen-van den Broek MW, van den Bogaardt AJ, et al. Age-dependent changes in geometry, tissue composition and mechanical properties of fetal to adult cryopreserved human heart valves. *PLoS ONE*. 2016;11(2):e0149020.
  57. Jana S, Lerman A, Simari RD. In vitro model of a fibrosa layer of a heart valve. *ACS Appl Mater Interfaces*. 2015;7(36):20012–20.
  58. Oomen PJ, Loerakker S, van Geemen D, Neggers J, Goumans MT, van den Bogaardt AJ, et al. Age-dependent changes of stress and strain in the human heart valve and their relation with collagen remodeling. *Acta biomaterialia*. 2015;29:161–9.
  59. Baker BM, Gee AO, Metter RB, Nathan AS, Marklein RA, Burdick JA, et al. The potential to improve cell infiltration in composite fiber-aligned electrospun scaffolds by the selective removal of sacrificial fibers. *Biomaterials*. 2008;29(15):2348–58.
  60. Zhong S, Zhang Y, Lim CT. Fabrication of large pores in electrospun nanofibrous scaffolds for cellular infiltration: a review. *Tissue Eng Part B Rev*. 2012;18(2):77–87.
  61. Wong E, Parvin Nejad S, D'Costa KA, Machado Siqueira N, Lecce M, Santerre JP, et al. Design of a mechanobioreactor to apply anisotropic, biaxial strain to large thin biomaterials for tissue engineered heart valve applications. *Ann Biomed Eng*. 2022;50:1073–89.
  62. Syedain ZH, Tranquillo RT. Controlled cyclic stretch bioreactor for tissue-engineered heart valves. *Biomaterials*. 2009;30(25):4078–84.

## Publisher's Note

Springer Nature remains neutral with regard to jurisdictional claims in published maps and institutional affiliations.

Ready to submit your research? Choose BMC and benefit from:

- fast, convenient online submission
- thorough peer review by experienced researchers in your field
- rapid publication on acceptance
- support for research data, including large and complex data types
- gold Open Access which fosters wider collaboration and increased citations
- maximum visibility for your research: over 100M website views per year

At BMC, research is always in progress.

Learn more [biomedcentral.com/submissions](https://biomedcentral.com/submissions)

